Glycocalyx-Mimicking Nanoparticles for Stimulation and Polarization of Macrophages via Specific Interactions

Lu Su, Weiyi Zhang, Xiulong Wu, Yufei Zhang, Xi Chen, Guangwei Liu, Guosong Chen, and Ming Jiang*

***M**alignant tumors develop multiple mechanisms to impair and escape from antitumor immune responses, of which tumor-associated macrophages that often show immunosuppressive phenotype (M2), play a critical role in tumor-induced immunosuppression. Therefore, strategies that can reverse M2 phenotype and even enhance immune-stimulation function of macrophage would benefit tumor immunotherapy. In this paper, self-assembled glyco-nanoparticles (glyco-NPs), as artificial glycocalyx, have been found to be able to successfully induce the polarization of mouse primary peritoneal macrophages from M2 to inflammatory type (M1). The polarization change was evidenced by the decreased expression of cell surface signaling molecules CD206 and CD23, and the increased expression of CD86. Meanwhile, secretion of cytokines supported this polarization change as well. More importantly, this phenomenon is observed not only in vitro, but also in vivo. As far as we known, this is the first report about macrophage polarization being induced by synthetic nanomaterials. Moreover, preparation, characterization of these glyco-NPs and their interaction with the macrophages are also demonstrated.*

1. Introduction

With the ever-expanding possibilities to build supramolecular structures, chemists are challenged to mimic nature in which construction of artificial cells and realization of their functions has been one of the most attractive tasks.[1] Till now, macromolecular self-assembly has been quite an important strategy used by chemists aiming at artificial cell[2] due to the stability and functionality of the self-assembled polymeric structures in a scale range from nanometer to millimeter. Compared with the successful mimicking of cells with intracellular compartments (the organelles) and concerted enzymatic reactions, wherein[3] only a few reports focused on mimicking the cell surface structure, e.g., glycocalyx, a heavy layer of sugars containing glycoprotein, glycolipid, and proteoglycan covering the surface of all types of cells.[4] The glycocalyx on leukocytes is regarded as important for their migration and interaction with endothelial cells of blood vessel. To this goal, polymeric materials exhibit virtues providing a scaffold to mimic the cell membrane as well as the dense polymeric sugar layer simultaneously.

The role of glycocalyx in infection, inflammation, and cancer has been progressively revealed in literature.[5] Among these, immunological function is an indispensable one, which to some extent was overlooked before in the study of mimicking glycocalyx. Macrophages (Mϕ) are a type of innate immune cells with critical roles in innate immune response to invading organisms, including inflammation, pathogen

Dr. L. Su, W. Zhang, X. Wu, Y. Zhang, Prof. G. Chen, Prof. M. Jiang
The State Key Laboratory of Molecular Engineering of Polymers, Collaborative Innovation Center of Polymers and Polymer Composite Materials and Department of Macromolecular Science
Fudan University, Shanghai 200433, China
E-mail: guosong@fudan.edu.cn
X. Chen, Prof. G. Liu
Department of immunology
School of Basic Medical Sciences
Fudan University, Shanghai 200032, China

DOI: 10.1002/smll.201403838

elimination, and coordination of the adaptive immune response.[6] The function of Mϕ[7] is greatly related to cell–cell interactions mediated *via* ligand-receptor on their surface, in which protein–glycan interaction, participated by proteins (or lectins) with carbohydrate-recognition domains (CRDs) found on the surface of Mϕ and the glycocalyx on the interacting cell, is involved.[8]

Macrophages are scavengers of the immune system. These cells reside in every tissue in the body where they engulf apoptotic cells and pathogens, and produce immune effector molecules. Macrophages are remarkably plastic cells and can change their functional phenotype depending on the environmental cues they receive. These cues are provided by cell–cell contact and secretary cytokines. And polarized macrophages can be broadly classified into classically activated macrophages (or M1), an immunostimulatory phenotype, and alternatively activated macrophages (or M2), an immunomodulatory phenotype. Recent research results emphasize that the roles of Mϕ greatly rely on their polarization, which is performed by the expression of different cell surface molecules and cytokines secretion.[9] For example, a protective role in tumorigenesis has been ascribed to M1ϕ, which activates tumor-killing mechanisms and suppresses the function of tumor-associated macrophages (M2 phenotype).[10] Considering the plasticity of Mϕ, strategies that polarize macrophages from M2ϕ to M1ϕ recently are employed in cancer immunotherapy.[11] However, until now to the best of our knowledge, this polarization change has not been achieved under the stimulation of supramolecular assemblies.

Herein, the effect of glycocalyx-mimicking nanoparticles (glyco-NPs) on macrophage activation and polarization *via* cell interaction is explored for the first time on primary mouse peritoneal macrophages (pMϕ). First, the binding of glyco-NPs on pMϕ was proved to be receptor-dependent, showing that the uptake of glyco-NPs by the pMϕ required specific receptors on cell surface. Then expression of cell surface molecules and cytokine secretion demonstrated the polarization change of pMϕ from M2ϕ to M1ϕ, stimulated by the artificial glycocalyx assembly. Moreover, the effect was observed not only in vitro, but also in vivo. Considering the low toxicity and synthetic nature of glyco-NPs, we anticipate this work brings them great potential in antitumor immunotherapy.

2. Results and Discussion

2.1. Design of Self-Assembled Glyco-NPs

In our previous study, glyco-NPs were employed to mimic glycocalyx with different sugar regio-isomers and stereoisomers on cell surfaces,[12] we found that glyco-isomerism has strong effects on the function and intracellular pathway of the nanoparticles. For example, the glyco-NPs covered with galactoside linked via anomeric position reached lysosome via early endosome and late endosome of Hep G2 cells, while the isomer linked via 6-position (C-6) only reached and stopped at early endosome. This result indicates that glyco-NPs may have unique functions that are not predictable from its oligosaccharide analogues and glycopolymer chains.[13,14] To understand the discrepancies, the current study focuses on the specific binding of the glyco-NPs to the receptors on pMϕ and the following events including endocytosis and the immune responses. Particularly, the effect of glyco-NPs on polarization change of Mϕ, which is related to cancer therapy, yet remained unexplored before, is analyzed.

In this study, block copolymers with a hydrophobic block polystyrene (PS) and hydrophilic glyco-block (PR) are employed to self-assemble into glyco-NP with an inert organic core PS and a glycopolymer shell (**Scheme 1**). Despite its synthetic convenience, in this study, inorganic nanoparticle was not used to construct the core, since inorganic nanomaterials may also induce immune response.[15] Using post-polymerization strategy, D-galactopyranoside (α:β = 5:1), α-D-mannopyranoside and L-fucopyranoside (α:β = 8:1) were connected to the same kind of polymeric chain as pedant groups to afford fluorescent block copolymers **F-PGal-*b*-PS**, **F-PMan-*b*-PS**, and **F-PFuc-*b*-PS**, respectively (Scheme 1), which ensured the same molecular weight, block ratio, and polydispersity of these polymers. Selection of the three sugars is related to presentation of C-type lectins, the most important lectin family on Mϕ,[16] i.e., macrophage galactose lectin (MGL, CD301) with specificity to galactopyranoside (Gal),[17] and mannose receptor (MR, CD206) specific to mannopyranoside (Man) and fucopyranoside (Fuc).[18] Moreover, MGL and MR represent two typical species of C-type lectins expressed on immune cells. MGL is a cluster of three CRDs supported by a coiled-coil peptide stem; while the multiple CRDs of MR are at the side of a rigid stem.[19] Thus one important aim of the current study is to evaluate the uptake of glyco-NPs with different sugars by pMϕ in the presence of MGL and MR, and their sequential immune responses. As control, biocompatible nanoparticles with oligoethylene glycol (OEG) as the shell and PS core, which has high aqueous solubility and stability in physiological solutions similar to glyco-NPs, were prepared *via* the same strategy.

2.2. Synthesis of Fluorescent-Labeled Block Copolymers

To visualize the glyco-NPs under fluorescence microscope, fluorescein was designed to covalently attach to glycopolymers (Scheme S1, Supporting Information). The fluorescent-labeled block glycopolymers were synthesized via two-step RAFT polymerization followed by postpolymerization modification. The results of the polymerization are shown in **Table 1** The degree of polymerization (DP) of poly(glycidyl methacrylate) (**PG**) was found to be 25 by comparing the intensity of phenyl group at δ 7.0–8.0 ppm from RAFT agent and that of epoxy units at 3.22 ppm in the ^{1}H NMR spectrum (Figure S1, Supporting Information). Similarly, by comparing the intensity of PS at 6.5–7.5 ppm and that of epoxy units (Figure S1, Supporting Information), the DP of PS block of **PG-*b*-PS** was found to be 325. Based on previous study,[20] this block length was selected to ensure the formation of nanoparticles with suitable diameter for biomedical

DOI: 10.1002/smll.201403838

small NANO MICRO

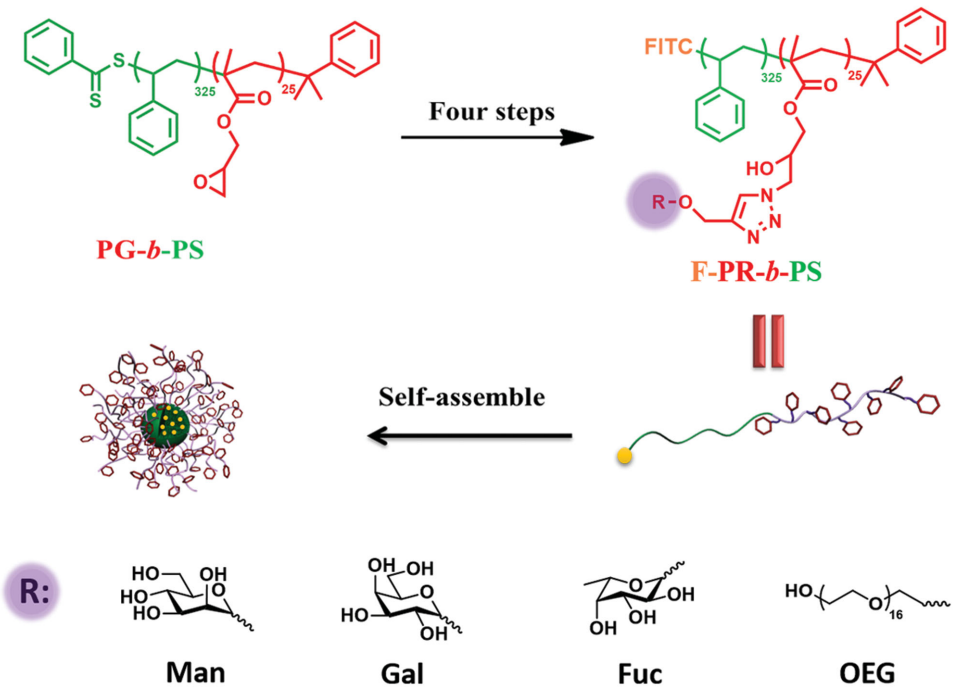

Scheme 1. Design and self-assembly of glycopolymers (**F-PMan-*b*-PS**, **F-PGal-*b*-PS**, **F-PFuc-*b*-PS**) and their nonsugar analogue **F-POEG-*b*-PS** to form glyco-NPs (**M-Man**, **M-Gal**, **M-Fuc**) and **M-PEG**.

study. Fluorescein was introduced to the end of $\mathbf{PG_{25}}$-*b*-$\mathbf{PS_{325}}$ via clicking *N*-(5-fluoresceinyl) maleimide to the polymer end group after reduction of the benzodithioate to thiol. The resultant $\mathbf{F\text{-}PG_{25}}$-*b*-$\mathbf{PS_{325}}$ was treated with NaN_3 for epoxide ring opening to afford $\mathbf{F\text{-}PGA_{25}}$-*b*-$\mathbf{PS_{325}}$. The complete transformation from epoxide to azide was supported by the appearance of the methylene peak close to the azido moiety at 3.48 ppm (Figure S1, Supporting Information). The introduction of azido unit was also confirmed by Fourier transform infrared spectroscopy (FT-IR) analysis. In the spectrum of $\mathbf{F\text{-}PGA_{25}}$-*b*-$\mathbf{PS_{325}}$ (Figure S2, Supporting Information), a strong peak at 2105 cm^{-1} corresponding to the asymmetric stretching of the azido group was observed. After click reaction with different sugar alkynes, complete conversion to $\mathbf{F\text{-}PMan_{25}}$-*b*-$\mathbf{PS_{325}}$ and other glycopolymers was again confirmed by FT-IR (Figures S2 and S3, Supporting Information). Gel permeation chromatography (GPC) was employed to characterize the polymers in each step showing unimodal distributions with narrow polydispersity (PD.I. < 1.20) in Figures S4 and S5, Supporting Information. Similarly, nonglycopolymer $\mathbf{F\text{-}POEG_{25}}$-*b*-$\mathbf{PS_{325}}$ was prepared via the same method as control.

Table 1. M_n and PDI of fluorescent-labeled block copolymers and their precursors.

Polymers[a)]	M_n (^{1}H NMR)	M_n (GPC)[b)]	M_w/M_n (GPC)
PG_{25}	3 700	1600	1.20
PG_{25}-*b*-PS_{325}	37 500	16 700	1.16
F-PG_{25}-*b*-PS_{325}	37 800	17 000	1.15
F-PGA_{25}-*b*-PS_{325}	38 900	17 900	1.15
F-$PMan_{25}$-*b*-PS_{325}	44 300	26 000	1.19
F-$PGal_{25}$-*b*-PS_{325}	44 300	26 400	1.18
F-$PFuc_{25}$-*b*-PS_{325}	44 300	26 300	1.19
F-$POEG_{25}$-*b*-PS_{325}	60 100	33 600	1.20

[a)]Calculated from M_n obtained in ^{1}H NMR; [b)]PEG as calibration standard.

2.3. Self-Assembly of Glycopolymers into Glyco-NPs and their Characterization

Glyco-NPs were prepared by addition of water (4 mL) into 1 mL of dimethylacetamide (DMAc) solution of the glycopolymers (4 mg mL^{-1}). After dialysis, glyco-NPs formed with PS as the core and soluble glycopolymer as the shell, which were stable enough for further characterization and biological studies. Dynamic light scattering (DLS) measurements showed that diameters of glyco-NPs vary from 34 to 36 nm with narrow distributions (PD.I. < 0.1), which is suitable for possible nanotherapy applications,[21] (**Table 2**, **Figure 1**a and Figure S6, Supporting Information). Transmission electron microscopy (TEM) images confirmed their morphology as nanoparticles. Neutral surface property (–2.81 to –5.01 mV) of these glyco-NPs in PBS buffer (pH 7.4) was also confirmed by Zeta potential measurements. In addition, the successful modification of fluorescein was supported by fluorescent spectra (Figure S7D, Supporting Information). For clarities, the glyco-NPs are respectively marked as **M-Man**, **M-Gal**, and **M-Fuc**, according to their glycopolymer block. All of their characterizations are listed in Table 2 and Figures S6–S8, Supporting Information, while the DLS and TEM data of **M-Man** are shown in Figure 1 as a representative. Nanoparticle

DOI: 10.1002/smll.201403838

Table 2. Characterization of glyco-NPs.

Glycopolymers	Glyco-NPs	Diameter [D_h]	PD.I.	ξ[a)]
F-PMan$_{25}$-*b*-PS$_{325}$	M-Man	34	0.04	−3.62
F-PGal$_{25}$-*b*-PS$_{325}$	M-Gal	36	0.05	−4.03
F-PFuc$_{25}$-*b*-PS$_{325}$	M-Fuc	34	0.06	−4.40
F-POEG$_{25}$-*b*-PS$_{325}$[b)]	M-PEG	55	0.09	−2.81

[a)]Measured in PBS buffer (pH 7.4, 20×10^{-3} M) at room temperature; [b)]Nonglycopolymer control.

M-PEG was prepared by block copolymer **F-POEG-*b*-PS** as control without any glyco-components (Table 2 and Figures S6–S8, Supporting Information).

2.4. *In Vitro* Binding of Glyco-NPs to pMϕ at 4 °C and the Inhibition Assay

Considering the lack of immune activities in the current available cell line RAW264.7, primary mouse pMϕ were used to measure the binding of glyco-NPs in vitro (Figure S9, Supporting Information). In this paper, unless specifically mentioned, the pMϕ are harvested from mice with pretreatment of thioglycollate broth (TG), which is a general procedure in immunology study (see the Supporting Information). PMϕ were harvested and analyzed by fluorescence-activated cell sorting (FACS) for surface expression of F4/80, which is a useful marker for Mϕ. First, MTT assay showed no cytotoxicity of glyco-NPs (<1×10^{-6} M) to pMϕ (Figure S10, Supporting Information). In order to exclude nonspecific phagocytosis, the binding tests of glyco-NPs to pMϕ as a function of nanoparticle dose and incubation time were performed at 4 °C in which only specific binding instead of engulfing could occur. Normalization of the mean fluorescence intensity (MFI) of each type of the glyco-NPs was performed for the quantitative measurements by flow cytometry (FCM). As shown in **Figure 2**a, at a fixed incubation time of 60 min, the MFI of the cells with different glyco-NPs increased almost linearly along the increase of nanoparticle concentration. When the particle concentration was fixed at 1×10^{-6} M, their cellular binding increased significantly along the incubation time, from 15 to 60 min (Figure 2b). Thus, the culture condition of 1×10^{-6} M and 60 min were adapted for the following experiments. As control, the MFI remained constant for incubation with **M-PEG**. This indicates that the binding of glyco-NPs to pMϕ could be attributed to their sugar surfaces. As shown in Figure 2a,b, the MFI of **M-Gal** was much higher than those of **M-Fuc** and **M-Man** at the same dose and incubation time, indicating a stronger binding of the former than the latter ones to pMϕ.

To prove the binding specificity, free sugars and the respective block antibodies of MGL (MGL mAb, anti-CD301) and MR (MR mAb, anti-CD206) are selected to inhibit the interaction between glyco-NPs and pMϕ. Typically, before the incubation of pMϕ with **M-Gal**, the cells were first treated with free galactose or anti-CD301 antibody for 1 h. Significant inhibition of the binding of pMϕ with **M-Gal**, by either galactose and anti-CD301 antibody, was observed as shown in Figure 2c,d, respectively. Similarly, the binding of **M-Fuc** and **M-Man** to pMϕ was also strikingly inhibited by free fucose and mannose, respectively (Figure 2c). However, the binding of glyco-NPs to pMϕ could not be effectively inhibited by anti-CD206 antibody, showing the remarkable binding ability of **M-Fuc** and **M-Man** to pMϕ, which could be possibly explained by the multivalent effect between the glyco-NP and CD206.[22] We suppose that it is possible that this effect is much more enhanced on CD206 than that on CD301, due to the different orientation of CRDs of the former[23] than the latter.

2.5. The Specific Receptor-Dependent uptake of Glyco-NPs by pMϕ at 37 °C

The glyco-NPs were further incubated with pMϕ at 37 °C for 2 h. As shown in Figure S11, Supporting Information, as expected, the MFI of pMϕ after incubation with **M-Man** at 37 °C was much higher than that at 4 °C. It is known that the extracellular substances can be transported into cells through several different pathways such as trans-membrane diffusion, phagocytosis and receptor-mediated or nonspecific endocytosis.[24] To determine the uptake mechanisms of pMϕ to glyco-NPs at 37 °C, special inhibitors were selected to treat

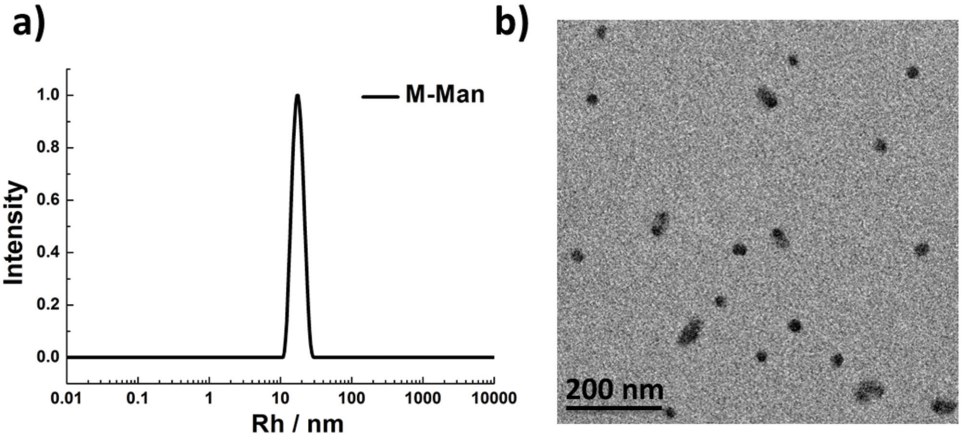

Figure 1. a) DLS and b) TEM characterization of **M-Man**.

DOI: 10.1002/smll.201403838

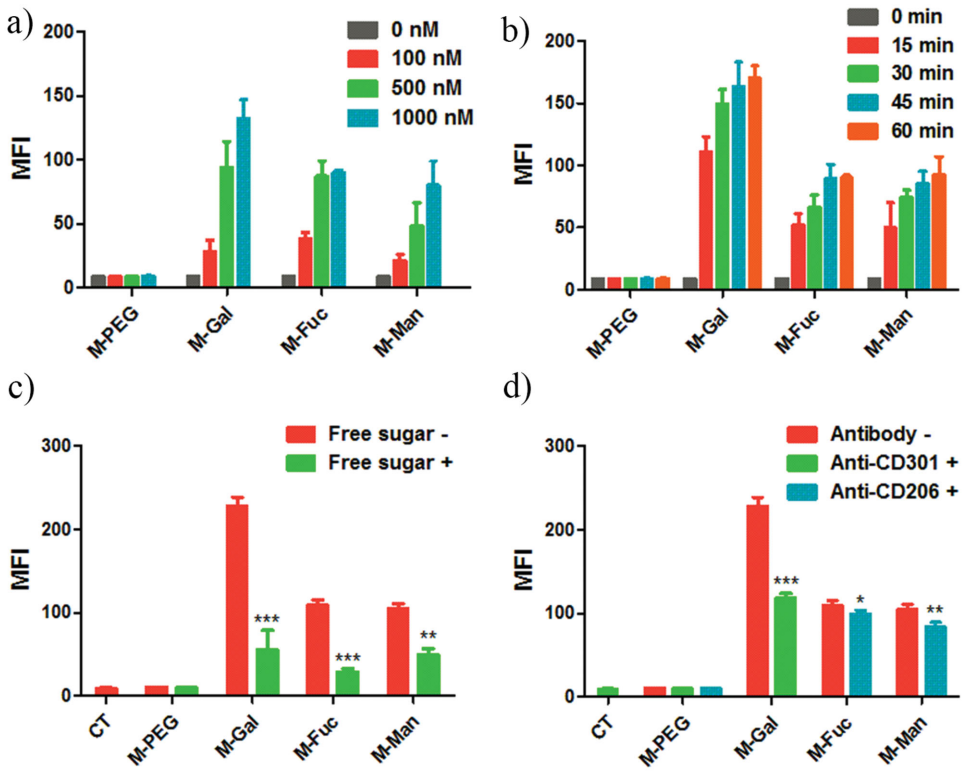

Figure 2. a) Dose dependence and b) time dependence of the binding of glyco-NPs and **M-PEG** to pMϕ at 4 °C. Inhibition studies to the binding of glyco-NPs by pMϕ with c) free sugar d) and antibodies at 4 °C. Data are expressed as the mean ± SD of three independent experiments. * $p < 0.05$, ** $p < 0.01$, and *** $p < 0.001$.

the cells before incubation with the particles: Cytochalasin D (CytD) leads to the depolymerization of actin filaments, which primarily inhibits macropinocytosis.[25] Sucrose inhibits clathrin-mediated endocytosis, while methyl-β-cyclodextrin blocks the caveolae-mediated endocytosis pathway.[26] As shown in **Figure 3** the uptake efficiency of pMϕ to glyco-NPs was significantly decreased after pretreatment of sucrose or methyl-β-cyclodextrin. While pretreatment of CytD decreased the uptake of **M-Man**, no significantly influence on that of **M-Gal** and **M-Fuc** was observed. The result suggested that the uptake of glyco-NPs by pMϕ at 37 °C was mainly relied on clathrin- and caveolae-mediated endocytosis, indicating the dominance of receptor-mediated process, which is consistent to the previous inhibition test at 4 °C.

Localization of glyco-NPs after internalization was then investigated by confocal laser scanning microscopy (CLSM). PMϕ were subsequently treated with FITC-labeled glyco-NPs (green),APC-labeled anti-CD301 (red, **Figure 4**a) or anti-CD206 (red, Figure 4b) as well as lyso-tracker blue DND (blue). The lyso-tracker located lysosome, while the different antibodies tracked the corresponding receptors, which were internalized with the glyco-NPs by pMϕ. As shown in Figure 4 the CLSM images in different columns from left to right showed lysosomes stained with lyso-tracker blue DND

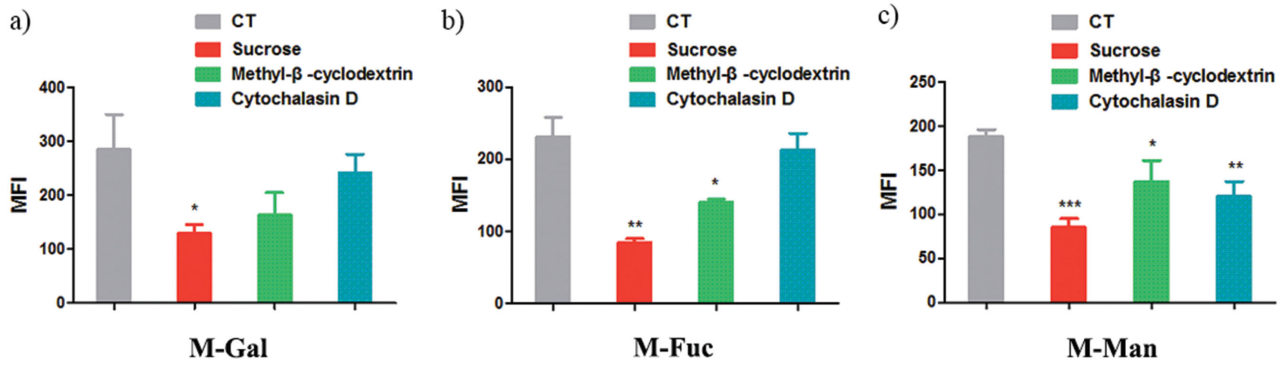

Figure 3. Inhibition test of a) **M-Gal**, b) **M-Fuc**, and c) **M-Man**. Methyl-β-cyclodextrin (20×10^{-3} M), sucrose (0.45 M) or cytochalasin D (3×10^{-3} M) were added 1 h before the addition of glyco-NPs. Non-treated cells were used as control. Data are expressed as the mean ± SD of three independent experiments. * $p < 0.05$, ** $p < 0.01$ and *** $p < 0.001$.

DOI: 10.1002/smll.201403838

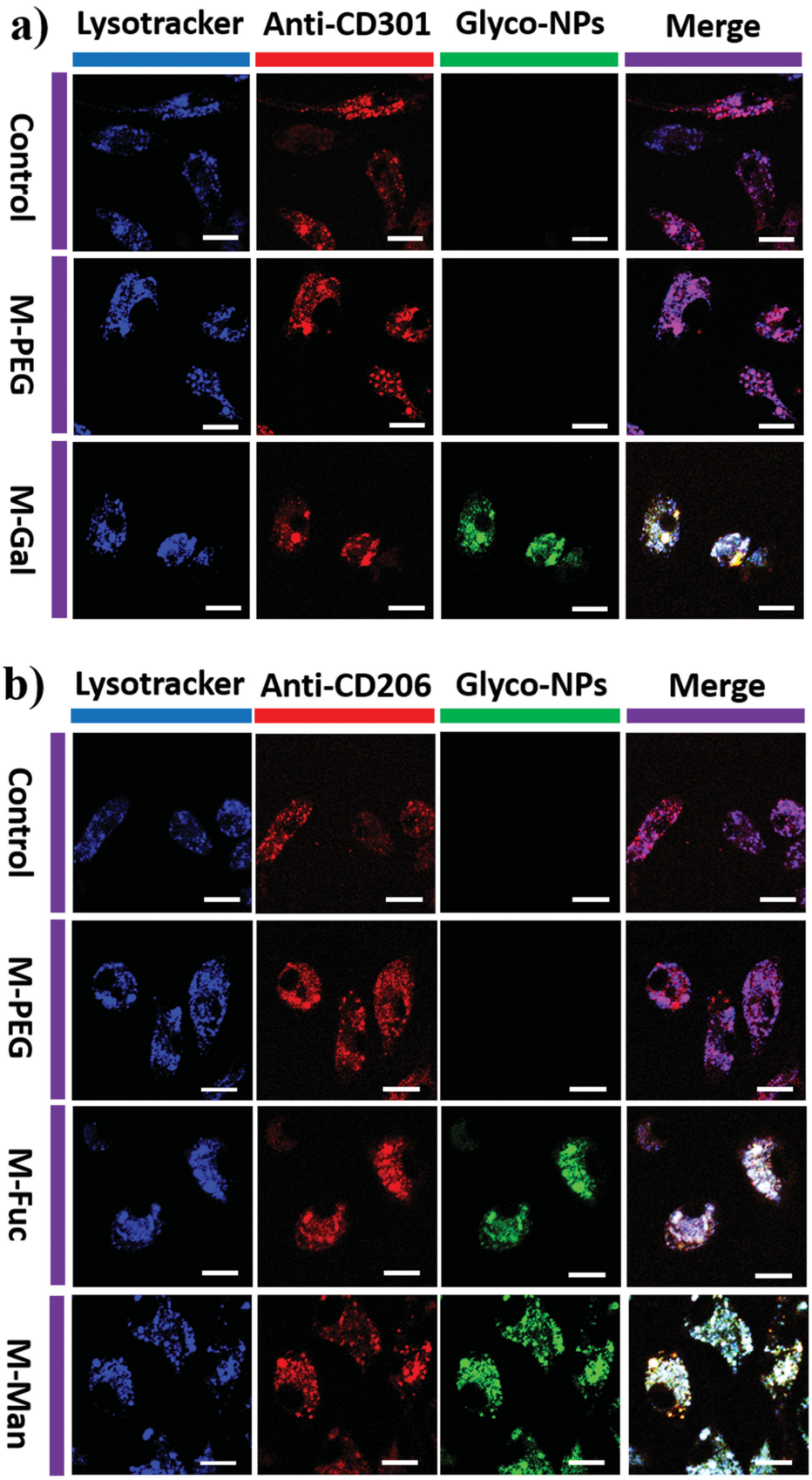

Figure 4. CLSM images of pMφ incubated with glyco-NPs or **M-PEG**. In each panel, images from left to right display lysosomes stained by lysotracker blue DND (blue), a) MGL or b) MR stained by their antibodies (red), glyco-NPs (green) in cells and overlay of the three images. The scale bars correspond to 10 μm in all the images.

small 2015,
DOI: 10.1002/smll.201403838

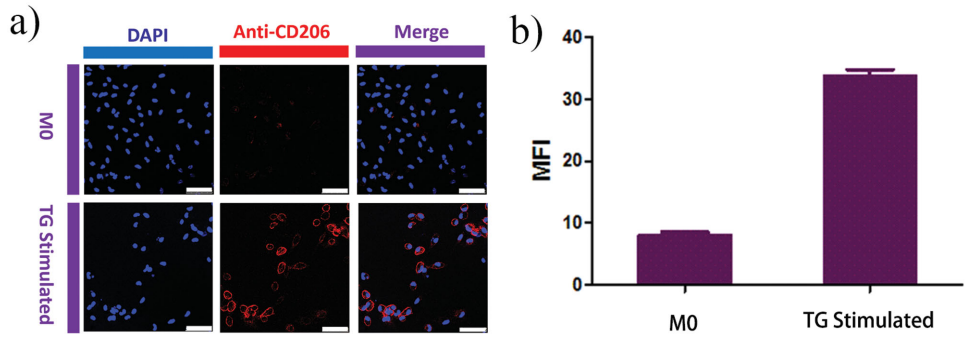

Figure 5. a) CLSM images of naïve pMφ (M0ϕ) and pMϕ harvested after TG stimulation (M2ϕ). Incubation with anti-CD206 antibody (red) showed the expression of CD206 after TG stimulation. The scale bars correspond to 50 μm in all the images. b) Flow cytometric analysis of expression of CD206 on M0 type pMφ and TG stimulated pMφ. Data are expressed as the mean ± SD of three independent experiments.

(blue), receptors stained with APC-labeled anti-CD301 antibody or anti-CD206 antibody (red) and internalized glyco-NPs labeled with fluorescein (green). On the right column, the merged images exhibit bright white color of **M-Fuc**, **M-Man**, and **M-Gal**, indicating the overlay of the colors of blue, red, and green. This result strongly evidenced the colocalization of lysosome, corresponding receptors to sugars (MGL or MR) and the glyco-NPs. As control, such green color was not observed in cells with **M-PEG**, confirming the specific receptor-dependent uptake.

2.6. M1 Polarization of pMϕs after the Uptake of Glyco-NPs *In Vitro*

Naïve pMϕ harvested from mice without any stimulators are ascribed as M0ϕ while TG stimulated ones used in this paper are generally considered as M2ϕ, which can be confirmed by the high expression of CD206, a useful marker for M2ϕ.[27] As shown in **Figure 5**a, compared to the naïve pMϕ, the expression of CD206 in TG-stimulated M2ϕ was quite high, which was obvious by using APC-conjugated anti-CD206 antibody under CLSM. Quantification analysis of CD206 expression (Figure 5b) from FACS supported the results from CLSM. To investigate the immunological effect of the glyco-NPs on pMϕ polarization, reference systems were employed in which the cells were treated with lipopolysaccharide (LPS) and Interleukin 4 (IL-4) in parallel. LPS and IL-4 are the classical stimulators to induce the polarization of pMϕ to M1 and M2, respectively. Typically pMϕ were first treated with glyco-NPs or the classical stimulators for 36 h, followed by incubation with the antibodies to different cell surface markers: CD86 were chosen as a typical marker for M1ϕ, while CD206 and CD23 were for M2ϕ. Then FACS experiment was performed to quantify the expression of these markers. In this experiment, TG-stimulated pM2ϕ harvested as the previous experiments were used. First the plasticity of Mϕ is demonstrated by using the classical stimulators. As shown in **Figure 6** expression of CD86 was increased on pM2ϕ treated with LPS, while level of CD206 and CD23 were decreased, suggesting a typical characteristic of M1ϕ, indicating the polarization of M2 to M1; while pM2ϕ with IL-4 stimulation remained the character of M2ϕ. Interestingly, the expression of CD86 on pM2ϕ incubated with different glyco-NPs was significantly upgraded, while their expression of CD206 and CD23 downgraded. This tendency, which is similar to that induced by LPS, but not IL-4, indicate the polarization of pMϕ from M2 to M1. As far as

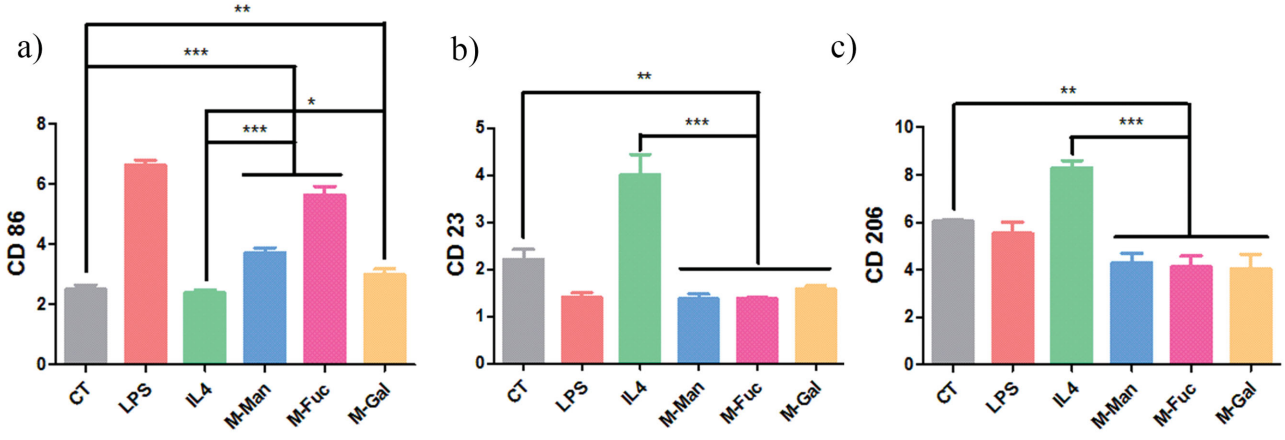

Figure 6. Glyco-NPs increased expression of CD86 and decreased expression of CD23 and CD206. After stimulation with glyco-NPs, LPS or IL-4, pMϕ were analyzed by FACS for surface expression of a) CD86, b) CD23, c) CD206. LPS stimulated and IL-4 stimulated cells were used as control. Data are expressed as the mean ± SD of three independent experiments. * $p < 0.05$, ** $p < 0.01$, and *** $p < 0.001$.

DOI: 10.1002/smll.201403838

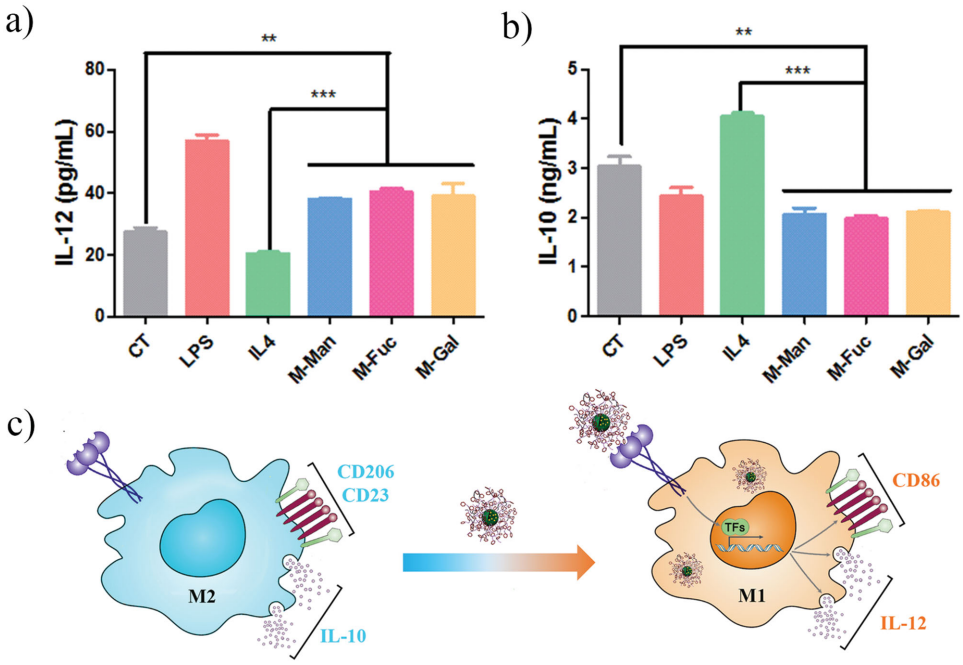

Figure 7. Glyco-NPs altered the cytokine secretion of pMϕ measured by ELISA. After stimulation with glyco-NPs, pMϕ were harvested and assayed for a) IL-12, b) IL-10. LPS stimulated and IL-4 stimulated cells were used as control. Data are expressed as the mean ± SD of three independent experiments. * $p < 0.05$, ** $p < 0.01$, and *** $p < 0.001$. c) Cartoon representation of Mϕ polarization change induced by glyco-NPs.

we know, this is the first observation of M1 polarization of pMϕ induced by artificial glycocalyx. The M1 polarization can be even more significant after treatment with **M-Fuc** than **M-Gal** and **M-Man**, indicated by the quite high expression of CD86. Moreover, this M1 polarization was further confirmed by cytokine secretion in enzyme-linked immunosorbent assay (ELISA). After incubation with glyco-NPs, pMϕ secreted higher level of Interleukin 12 (IL-12, a typical M1-type cytokine) and lower level of Interleukin 10 (IL-10, a typical M2-type cytokine) than those induced by IL-4 as well as the untreated ones (**Figure 7**a,b). This polarization change of pMϕ induced by glyco-NPs is also schematically illustrated in Figure 7c. It is worth to mention that the induction of M1 polarization by glyco-NPs was similar to the effect of LPS, but was much milder. This result is quite interesting as it is known that LPS always generates excess immune response, which may induce high toxicity and autoimmune diseases, thus we may expect that the glyco-NPs could be an immune adjuvant candidate with great potential.

2.7. *In Vivo* Uptake of Glyco-NPs by pMϕ and their Subsequent Polarization Tendency

To determine whether the uptake of glyco-NPs by pMϕ retained the same carbohydrate specificity in vivo, naïve mice were intraperitoneally (i.p.) injected with glyco-NPs. PMϕ were harvested at an indicated time following administration, and then were analyzed for the uptake of glyco-NPs. FACS data showed that the majority of those cells were pMϕ labeled by a macrophage cell-surface marker (APC Anti-F4/80). All of the different glyco-NPs were readily internalized by pMϕ as early as 30 min after injection (**Figure 8**). The number of internalized glyco-NPs by pMϕ was growing

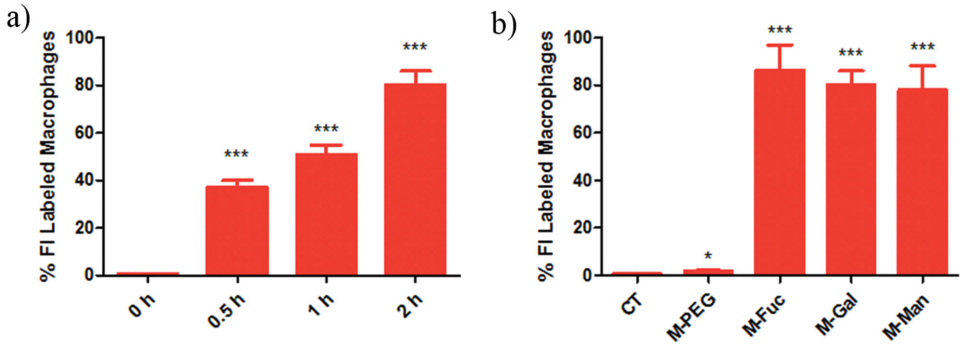

Figure 8. a) FACS results after i.p. injection with 200 µL M-Gal (FITC-labeled glyco-NPs and APC-labeled pMϕ). b) FACS results after i.p. injection of different glyco-NPs in 2 h. Data are expressed as the mean ± SD of three independent experiments. * $p < 0.05$, ** $p < 0.01$, and *** $p < 0.001$.

small 2015,
DOI: 10.1002/smll.201403838

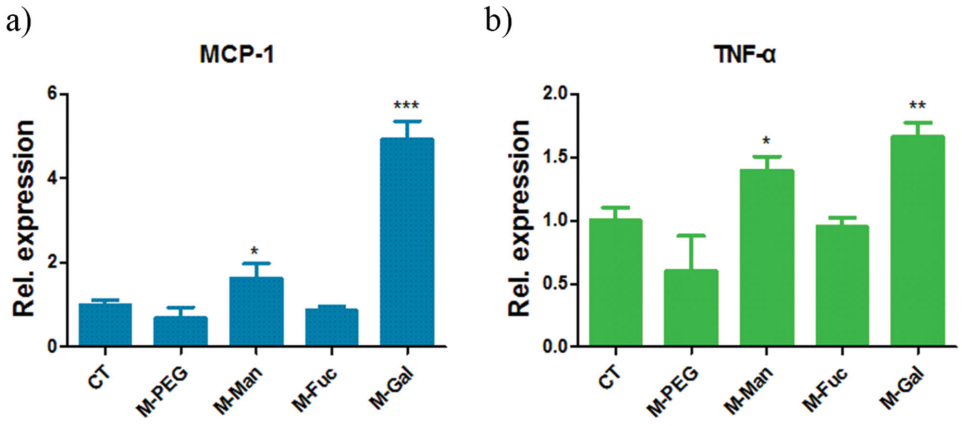

Figure 9. Q-PCR analyses of the expression of a) MCP-1 and b) TNF-α mRNA influenced by glyco-NPs *in vivo*. C57 mice were stimulated with TG, followed by i.p. injection of glyco-NPs. PMϕ were isolated 6 h after injection and their total RNA was isolated. Data are expressed as the mean ± SD of three independent experiments. * $p < 0.05$, ** $p < 0.01$, and *** $p < 0.001$.

increasingly along the incubation time. The results demonstrated that glyco-NPs indeed could be internalized by pMϕ in vivo, similar to the in vitro results.

To further evaluate the effect of glyco-NPs on polarization of pMϕ in vivo, mice were first injected with 3% TG solution followed by glyco-NPs. Then pMϕ were harvested and the cytokines released were analyzed by real time polymerase chain reaction (Q-PCR). Pro-inflammatory cytokines, tumor necrosis factor α (TNF-α) and monocyte chemotactic protein 1 (MCP-1), two characteristic cytokines to M1ϕ (Table S1, Supporting Information), were evaluated. Similar to the in vitro results, higher expression of TNF-α and MCP-1 was also observed after the injection of glyco-NPs (**Figure 9**), while no significant change with the M-PEG injection. TNF-α is produced chiefly by activated M1ϕ,[28] which plays important role in pathogen elimination. MCP-1 is one of the key chemokines that regulate migration and infiltration of Mϕ, which participates in inflammation and infection. It is also known that M1ϕ secreted significantly more MCP-1 compared with M2ϕ, which make MCP-1 an important marker for M1ϕ.[29] Thus the increased secretion of TNF-α and MCP-1 from pMϕ induced by glyco-NPs, also indicate polarization of pMϕ from M2 to M1 in vivo. This result was consistent to the in vitro results, showing that the M2 to M1 polarization effect induced by glyco-NPs was not only observed in vitro, but also in vivo.

3. Conclusion

In this study, three glyco-NPs were prepared and shown to specifically engage macrophages both in vitro and in vivo in a carbohydrate-dependent manner, which could be used as vehicles for carbohydrate-targeting therapeutic application. These glyco-NPs show much more sensitivity to the carbohydrate-specific receptors on Mϕ, compared to the glycopolymers reported in literature. Meanwhile, polarization from M2 to M1 could be induced both in vitro and in vivo by glyco-NPs as the first self-assembled material, proved by the expression of surface marker molecules and secretion of cytokines. This exhibits a bright future of glyco-NPs as new types of biomaterials with applications in immune adjuvants for cancer immunotherapy.

Supporting Information

Supporting Information is available from the Wiley Online Library or from the author.

Acknowledgements

Ministry of Science and Technology of China (Grant No. 2011CB932503), National Natural Science Foundation of China (Grant Nos. 21474020, 91227203 and 51322306), the Shanghai Rising-Star Program (Grant No. 13QA1400600), and the Innovation Program of the Shanghai Municipal Education Commission are acknowledged for their financial support.

[1] J. van der Weijden, L. E. Paulis, M. Verdoes, J. C. M. van Hest, C. G. Figdor, *Chem. Sci.* **2014**, *5*, 3355.
[2] a) Y. Zhao, F. Sakai, L. Su, Y. Liu, K. Wei, G. Chen, M. Jiang, *Adv. Mater.* **2013**, *25*, 5215; b) X. Xu, Y. Li, Y. Jian, G. Wang, B. He, Z. Gu, *Acta Polymerica Sinica* **2012**, 1128; c) L. W. Place, M. Sekyl, M. J. Kipper, *Biomacromolecules* **2014**, *15*, 680.
[3] M. Marguet, C. Bonduelle, S. Lecommandoux, *Chem. Soc. Rev.* **2013**, *42*, 512.
[4] a) J. Huang, C. Bonduelle, J. Thévenot, S. Lecommandoux, A. Heise, *J. Am. Chem. Soc.* **2012**, *134*, 119; b) L. Su, Y. Zhao, G. Chen, M. Jiang, *Polym. Chem.* **2012**, *3*, 1560.
[5] a) M. A. Wolfert, G. Boons, *Nat. Chem. Bio.* **2013**, *9*, 776; b) Y. van Kooyk, G. A. Rabinovich, *Nat. Immunol.* **2008**, *9*, 593; c) C. R. Becer, M. I. Gibson, J. Geng, R. Ilyas, R. Wallis, D. A. Mitchell, D. M. Haddleton, *J. Am. Chem. Soc.* **2010**, *132*, 15130.
[6] A. Chawla, K. D. Nguyen, Y. P. S. Goh, *Nat. Rev. Immunol.* **2011**, *11*, 738.
[7] D. M. E. Bowdish, M. S. Loffredo, S. Mukhopadhyay, A. Mantovani, S. Gordon, *Microbes Infect.* **2007**, *9*, 1680.
[8] K. Drickamer, *Curr. Opin. Struct. Biol.* **1999**, *9*, 585.
[9] A. Mantovani, S. Sozzani, M. Locati, P. Allavena, A. Sica, *Trends Immunol.* **2002**, *23*, 549.
[10] a) P. J. Murray, T. A. Wynn, *Nat. Rev. Immunol.* **2011**, *11*, 723; b) T. Sun, C. Ge, *Chin. J. Cancer Biother.* **2011**, *18*, 686.

[11] L. Bingle, N. J. Brown, C. E. Lewis, *J. Pathol.* **2002**, *196*, 254.
[12] P. Sun, Y. He, M. Lin, Y. Zhao, Y. Ding, G. Chen, M. Jiang, *ACS Macro Lett.* **2014**, *3*, 96.
[13] A. V. Chavez-Santoscoy, R. Roychoudhury, N. L. B. Pohl, M. J. Wannemuehler, B. Narasimhan, A. E. Ramer-Tait, *Biomaterials* **2012**, *33*, 4762.
[14] E. Song, M. J. Manganiello, Y. Chow, B. Ghosn, A. J. Convertine, P. S. Stayton, L. M. Schnapp, D. M. Ratner, *Biomaterials* **2012**, *33*, 6889.
[15] J. P. M. Almeida, A. Y. Lin, R. J. Langsner, P. Eckels, A. E. Foster, R. A. Drezek, *Small* **2014**, *10*, 812.
[16] Y. van Kooyk, G. A. Rabinovich, *Nat. Immunol.* **2008**, *9*, 593.
[17] C. Napoletano, I. G. Zizzari, A. Rughetti, H. Rahimi, T. Irimura, H. Clausen, H. H. Wandall, F. Belleudi, F. Bellati, L. Pierelli, L. Frati, M. Nuti, *Eur. J. Immunol.* **2012**, *42*, 936.
[18] U. Gazi, L. Martinez-Pomares, *Immunobiology* **2009**, *214*, 554.
[19] A. Varki, R. D. Cummings, J. D. Esko, H. H. Freeze, P. Stanley, C. R. Bertozzi, G. W. Hart, M. E. Etzler, *Essentials of Glycobiology*, Cold Spring Harbor Laboratory Press, Cold Spring Harbor, NY **2009**.
[20] a) L. Su, C. Wang, F. Polzer, Y. Lu, G. Chen, M. Jiang, *ACS Macro Lett.* **2014**, *3*, 534; b) Z. Li, Y. Liang, F. Li, *Chem. Commun.* **1999**, *16*, 1557.
[21] a) W. Jiang, B. Y. S. Kim, J. T. Rutka, W. Chan, *Nat. Nanotechnol.* **2008**, *3*, 145; b) F. Zhang, S. Zhang, S. F. Pollack, R. Li, A. M. Gonzalez, J. Fan, J. Zou, S. E. Leininger, A. Pavia-Sanders, R. Johnson, L. D. Nelson, J. E. Raymond, M. Elsabahy, D. M. P. Hughes, M. W. Lenox, T. P. Gustafson, K. L. Wooley, *J. Am. Chem. Soc.* **2015**, *137*, 2056.
[22] J. D. Badji , A. Nelson, S. J. Cantrill, W. B. Turnbull, J. F. Stoddart, *Acc. Chem. Res.* **2005**, *38*, 723.
[23] M. E. Taylor, K. Bezouska, K. Drickamer, *J. Biol. Chem.* **1992**, *267*, 1719.
[24] a) S. D. Conner, S. L. Schmid, *Nature* **2003**, *422*, 37; b) D. Yu, Y. Zhang, X. Zhou, Z. Mao, C. Gao, *Biomacromolecules* **2012**, *13*, 3272.
[25] a) C. Lamaze, L. M. Fujimoto, H. L. Yin, S. L. Schmid, *J. Biol. Chem.* **1997**, *272*, 20332; b) I. A. Khalil, K. Kogure, H. Akita, H. Harashima, *Pharmacol. Rev.* **2006**, *58*, 32.
[26] X. Hu, J. Hu, J. Tian, Z. Ge, G. Zhang, K. Luo, S. Liu, *J. Am. Chem. Soc.* **2013**, *135*, 17617.
[27] a) K. M. Choi, P. C. Kashyap, N. Dutta, G. J. Stoltz, T. Ordog, T. Shea Donohue, A. J. Bauer, D. R. Linden, J. H. Szurszewski, S. J. Gibbons, G. Farrugia, *Gastroenterology* **2010**, *138*, 2399; b) C. Liu, Y. Li, J. Yu, L. Feng, S. Hou, Y. Liu, M. Guo, Y. Xie, J. Meng, H. Zhang, B. Xiao, C. Ma, *PLoS ONE* **2013**, *8*, e54841.
[28] K. Pfeffer, *Cytokine Growth Factor Rev.* **2003**, *14*, 185.
[29] S. L. Deshmane, S. Kremlev, S. Amini, B. E. Sawaya, *J. Interferon Cytokine Res.* **2009**, *29*, 313.

Received: December 28, 2014
Revised: February 21, 2015
Published online:

DOI: 10.1002/smll.201403838